The Astrophysical Journal, 780:144 (10pp), 2014 January 10 doi:10.1088/0004-637X/780/2/144

PROPERTIES OF MAGNETIC HELICITY FLUX IN TURBULENT DYNAMOS

Ethan T. Vishniac[1] and Dmitry Shapovalov[2]
[1] Department of Physics and Engineering Physics, University of Saskatchewan, Saskatoon SK S7N 5E2, Canada; ethan.vishniac@usask.ca
[2] Department of Physics and Astronomy, Johns Hopkins University, 3400 N. Charles Street, Baltimore, MD 21218, USA; dmsh@jhu.edu
Received 2013 March 28; accepted 2013 October 28; published 2013 December 19

ABSTRACT

We study the flux of small-scale magnetic helicity in simulations of driven statistically homogeneous magnetohydrodynamic turbulence in a periodic box with an imposed large-scale shear. The simulations show that in the regime of strong dynamo action the eddy-scale magnetic helicity flux has only two significant terms: advective motion driven by the large-scale velocity field and the Vishniac–Cho (VC) flux which moves helicity across the magnetic field lines. The contribution of all the other terms is negligible. The VC flux is highly correlated with the large-scale electromotive force and is responsible for large-scale dynamo action, while the advective term is not. The VC flux is driven by the anisotropy of the turbulence. We derive analytical expressions for it in terms of the small-scale velocity or magnetic field. These expressions are used to predict the existence and strength of dynamo action for different turbulent anisotropies and tested against the results of the simulations.

Key words: ISM: general – magnetic fields – magnetohydrodynamics (MHD) – turbulence

Online-only material: color figures

1. INTRODUCTION

It is increasingly clear that magnetic helicity plays an important role in turbulent dynamos and the generation of large-scale cosmic magnetic fields (see Brandenburg 2005, for a review). The evolution of magnetic fields is tightly constrained by the conservation of magnetic helicity, which is a good approximation even in the presence of nonzero resistivity (Taylor 1974). Magnetic helicity is a measure of the links and twists in magnetic field $\mathbf{B}$ and is given by the volume integral of $\mathbf{A}\cdot\mathbf{B}$ (where $\mathbf{A}$ is the vector potential, $\mathbf{B}=\nabla\times\mathbf{A}$). Since the energy corresponding to a given magnetic helicity scales inversely with the scale of the twists, the magnetic helicity tends to accumulate at the largest scales, exhibiting an inverse cascade (Frisch et al. 1975). In astrophysical objects it decays on resistive time scales, much more slowly than magnetic energy, and is consequently almost independent of time (Berger 1984). The conservation of magnetic helicity, and the inverse cascade, are the underlying mechanism of the large-scale dynamo process, explaining the growth of magnetic field scale from eddy scales to the system scale.

Regions of nonzero magnetic helicity are created in cosmic objects by both small-scale turbulence and large-scale differential rotation and are readily observed (Démoulin et al. 2002; Lynch et al. 2005; Subramanian et al. 2006). Large-scale astrophysical magnetic fields have both poloidal and toroidal parts (Brandenburg & Subramanian 2005a), i.e., are necessarily helical. Turbulent motions transfer magnetic helicity between writhe and twist helicities and create many small-scale twists in the magnetic field. The Lorentz force due to these twists grows to suppress dynamo action (Sur et al. 2007). This process is called α-quenching and is a direct consequence of total magnetic helicity conservation. The magnitude of the large-scale magnetic fields limited by α-quenching has been estimated in several closure models (Pouquet et al. 1976; Kleeorin & Ruzmaikin 1982; Gruzinov & Diamond 1994; Blackman & Field 2002) and is orders of magnitude weaker than observed fields. Thus, at the very least this implies a need for small-scale magnetic helicity fluxes, which can remove helicity from the active dynamo regions and allow large-scale magnetic field to grow to observed magnitudes (Kleeorin et al. 2000). A more ambitious role for these fluxes was proposed by Vishniac & Cho (2001) who proposed that these fluxes drive the dynamo process directly through the accumulation of small-scale helicity with the required sign.

In the MHD limit, the conventional approach to the large-scale dynamo problem is through mean-field theory (MFT; Steenbeck et al. 1966). All quantities are divided into the mean (large-scale) and fluctuating (small-scale) parts, while various closure schemes provide estimates for the influence of small-scale quantities on the mean field. The goal of every closure scheme is to find the large-scale electromotive force (e.m.f.) $\mathcal{E}=\overline{\mathbf{v}\times\mathbf{b}}$, whose curl gives the time derivative of the large-scale magnetic field.

In our previous paper (Shapovalov & Vishniac 2011, hereafter SV11), we used periodic box simulations with a sinusoidal shear on the largest scale, a weak seed magnetic field and turbulence randomly and non-helically forced at small scales. In a periodic box (with no constant magnetic field), the volume integrated magnetic helicity is gauge invariant (Berger 1997). For a set of parameters close to the galactic dynamo, we observed a strong large-scale dynamo. Using these simulations we demonstrated that in differentially rotating object with strong large-scale dynamo the e.m.f. is highly correlated with accumulation of small-scale magnetic helicity, indicating that the turbulence drives a magnetic helicity flux, which then determines the parallel component of the e.m.f. (Equation (6) below). Furthermore, this correlation happens even in the absence of any large-scale magnetic field. This suggests that it would be interesting to study the magnetic helicity flux in more detail. At the same time, we found that the scale and orientation of the forcing (i.e., turbulence anisotropy) greatly influence the dynamo action, making the dynamo stronger or, alternatively, completely suppressing it. Consequently, it would be interesting to find how the magnetic helicity flux at small scales responds to changes in the location and orientation of the turbulent forcing.

Guided by results of SV11 and using the same numerical setup, this paper is devoted to further study of the properties of

the magnetic helicity flux, especially to isolating the components responsible for dynamo action and dynamo suppression. In Section 2 we introduce the small-scale magnetic helicity flux and derive expressions for the potentially important components in terms of small-scale magnetic or velocity fields. In Section 3 we explain our numerical method for driving MHD turbulence, set initial conditions, and show how we compute magnetic helicity flux terms. In Section 4 we discuss the results of our simulations. First, we analyze which terms contribute most to the dynamo action. This allows us to greatly simplify the small-scale magnetic helicity flux. Then we return to the analytical expressions from Section 2 and use them to predict approximately how the particular turbulence anisotropy (orientation of small-scale forcing) will influence the dynamo action. These predictions are compared with simulation results in Section 5. In Section 6 we give a summary of results and our conclusions. The Appendix is devoted to detailed derivations of certain terms of the small-scale magnetic helicity flux.

2. MAGNETIC HELICITY FLUX

In an incompressible conducting fluid the magnetic helicity flux is

$$\begin{aligned}\mathbf{J}_H &= (\mathbf{A}\cdot\mathbf{B})\,\mathbf{V} + \mathbf{B}\,(\Phi - \mathbf{A}\cdot\mathbf{V}) - \eta(\mathbf{A}\times\mathbf{J}) \\ &\equiv \mathbf{B}\Phi + \mathbf{A}\times(\mathbf{V}\times\mathbf{B}) - \eta(\mathbf{A}\times\mathbf{J}),\end{aligned} \tag{1}$$

where $\mathbf{V}$ is the velocity, $\mathbf{B}$ is the magnetic field divided by $(4\pi\rho)^{1/2}$, i.e., the Alfvén velocity. ρ is the density, Φ is the electric potential electric potential, $\mathbf{A}$ is the vector potential ($\mathbf{B} = \nabla\times\mathbf{A}$), $\mathbf{J} = \nabla\times\mathbf{B}$ is the current density, and η is the magnetic diffusivity. The magnetic helicity density $H^m = \mathbf{A}\cdot\mathbf{B}$ satisfies the equation:

$$\partial_t H^m + \nabla\cdot\mathbf{J}_H = -2\eta\mathbf{J}\cdot\mathbf{B}. \tag{2}$$

$\mathbf{V}$ and $\mathbf{B}$ satisfy the Navier–Stokes and induction equations, while the evolution of $\mathbf{A}$ is given by

$$\partial_t\mathbf{A} = (\mathbf{V}\times\mathbf{B}) - \nabla\Phi - \eta\mathbf{J}. \tag{3}$$

To remove the gauge ambiguity in $\mathbf{A}$ we use the Coulomb gauge $\nabla\cdot\mathbf{A} = 0$. When combined with the requirement that vector potential vanishes at infinity this implies

$$\mathbf{A}(\mathbf{r}) \equiv \int \frac{\mathbf{J}(\mathbf{r}')}{4\pi|\mathbf{r}-\mathbf{r}'|}\,d^3\mathbf{r}'. \tag{4}$$

This choice provides a direct connection between the magnetic helicity $\mathbf{A}\cdot\mathbf{B}$ and the current helicity $\mathbf{J}\cdot\mathbf{B}$, which is a physically measurable quantity. The unique advantage of this choice is that it maximizes the correlation between the two. Since the current helicity helps drive $\overline{\mathbf{v}\times\mathbf{b}}$, this means that this gauge choice is the only one which allows us to predict dynamo action from the evolution of the magnetic helicity. Taking the divergence of (3) leads to a constraint equation for Φ: $\triangle\Phi = \nabla\cdot(\mathbf{V}\times\mathbf{B})$.

The goal of this work is to follow the evolution of large-scale field quantities. With this in mind, let us denote the low-pass filtering operation with overbar (or angular brackets $\langle\,\rangle$ for longer expressions), so that $\overline{\mathbf{B}} \equiv \langle\mathbf{B}\rangle$ is a large-scale quantity (here – large-scale magnetic field) and $\mathbf{b} = (\mathbf{B} - \overline{\mathbf{B}})$ is a small-scale quantity. The operation can be defined arbitrarily; however, we will assume that $\overline{\overline{\mathbf{X}}\,\mathbf{y}} \approx 0$ for any double products and $\overline{\overline{\mathbf{X}}\,\overline{\mathbf{Y}}\,\mathbf{z}} \approx 0$ for any triple products, i.e., the vector fields $\mathbf{V}$ and $\mathbf{B}$ should have the "separation of scales" property. Similarly, we also assume that $\overline{\mathbf{X}\,\mathbf{Y}} - \overline{\overline{\mathbf{X}}\,\overline{\mathbf{Y}}} \approx 0$. Realistically, these relations will not be exactly satisfied for any choice of filters, but when the eddy scale is much smaller than the system size, they will be approximately satisfied for any reasonable filter definition.

The "large-scale magnetic helicity" is defined as $H_{\rm LS} = \overline{\mathbf{A}}\cdot\overline{\mathbf{B}}$ and corresponding large-scale flux is defined as $\mathbf{J}_{H_{\rm LS}} = \overline{\mathbf{B}}\overline{\Phi} + \overline{\mathbf{A}}\times(\overline{\mathbf{V}}\times\overline{\mathbf{B}} + \mathcal{E}) - \eta(\overline{\mathbf{A}}\times\overline{\mathbf{J}})$, where $\mathcal{E}$ is the turbulent e.m.f.: $\mathcal{E} = \overline{\mathbf{v}\times\mathbf{b}}$ and $\triangle\overline{\Phi} = \nabla\cdot(\overline{\mathbf{V}}\times\overline{\mathbf{B}} + \mathcal{E})$. Then the conservation equation for $H_{\rm LS}$ will be

$$\partial_t H_{\rm LS} + \nabla\cdot\mathbf{J}_{H_{\rm LS}} = 2\mathcal{E}\cdot\overline{\mathbf{B}} - 2\eta\overline{\mathbf{J}}\cdot\overline{\mathbf{B}}. \tag{5}$$

Although an important quantity in its own right, $H_{\rm LS}$ is largely driven by the behavior of the "small-scale magnetic helicity" $h = \overline{\mathbf{a}\cdot\mathbf{b}}$ and the inverse cascade. Regions of positive or negative magnetic helicity are created as systematic twists in structures at the scale of the turbulence. These twists are then moved around and transferred upward to the largest scales available, where the magnetic helicity is retained and dissipates slowly (Frisch et al. 1975; Brandenburg 2005). Subtracting (5) from the large-scale part of (2), we obtain the conservation equation for h:

$$\partial_t h + \nabla\cdot\mathbf{j}_{_H} \simeq -2\mathcal{E}\cdot\overline{\mathbf{B}} - 2\eta\overline{\mathbf{j}\cdot\mathbf{b}} \tag{6}$$

with the flux

$$\begin{aligned}\mathbf{j}_{_H} = {} & \overline{(\mathbf{a}\cdot\overline{\mathbf{B}})\mathbf{v}} + \overline{\mathbf{b}\phi_1} - \overline{(\mathbf{a}\cdot\mathbf{v})\overline{\mathbf{B}}} + \overline{(\mathbf{a}\cdot\mathbf{b})\overline{\mathbf{V}}} + \overline{\mathbf{b}\phi_2} - \overline{\mathbf{b}(\mathbf{a}\cdot\overline{\mathbf{V}})} \\ & + \overline{\mathbf{b}\phi_s} + \overline{\mathbf{a}\times(\mathbf{v}\times\mathbf{b})} - \eta(\overline{\mathbf{a}\times\mathbf{j}}),\end{aligned} \tag{7}$$

where $\triangle\phi_1 = \nabla\cdot(\mathbf{v}\times\overline{\mathbf{B}})$, $\triangle\phi_2 = \nabla\cdot(\overline{\mathbf{V}}\times\mathbf{b})$, and $\triangle\phi_s = \nabla\cdot(\mathbf{v}\times\mathbf{b} - \overline{\mathbf{v}\times\mathbf{b}})$.

Equation (6) shows that in the absence of resistivity and for a stationary concentration of small-scale magnetic helicity the parallel component of the e.m.f. is proportional to the divergence of the magnetic helicity flux. It means that supposed quenching of the e.m.f. and the growth of large-scale magnetic field lies in the particular properties of the flux (7). The validity of (6), i.e., the strong correlation between left- and right-hand parts of the equation was verified earlier in numerical simulations (SV11). An expression with the same terms as in (7), but split in a different way, was also obtained by Subramanian & Brandenburg (2006).

The first two terms in (7) were originally evaluated by Vishniac & Cho (2001); they form the Vishniac–Cho (VC) flux, additionally studied by Brandenburg & Subramanian (2005b) and Sur et al. (2007). The third term, $\overline{(\mathbf{a}\cdot\mathbf{v})\overline{\mathbf{B}}}$, is generally less interesting in mean-field dynamos, since it involves motion of magnetic helicity along the large-scale magnetic field lines. Similarly, the fourth term, $\overline{(\mathbf{a}\cdot\mathbf{b})\overline{\mathbf{V}}}$, is responsible for moving magnetic helicity with the large-scale velocity. However, this term may provide advection of small-scale magnetic helicity beyond the boundaries of dynamo region via large-scale outflow, e.g., galactic fountain or wind (Shukurov et al. 2006). The terms $\overline{\mathbf{b}\phi_s}$ and $\overline{\mathbf{a}\times(\mathbf{v}\times\mathbf{b})}$ can be ignored in this study, because their dominant contribution to the magnetic helicity flux is a function only of the local properties of the turbulence. In a homogeneous system, like the one we study here, this implies that they do not contribute to the magnetic helicity flux divergence. They may play an important role in vertically stratified systems.

The first two terms in (7) can be rewritten as an integral over correlations, i.e.,

$$\langle(\mathbf{a}\cdot\overline{\mathbf{B}})\mathbf{v}\rangle+\langle\mathbf{b}\phi_1\rangle=\left\langle\int\frac{d^3\mathbf{r}'}{4\pi r'}(\mathbf{v}(\mathbf{r})\overline{\mathbf{B}(\mathbf{r})}\cdot\mathbf{j}(\mathbf{r}+\mathbf{r}')-\mathbf{b}(\mathbf{r})\nabla\cdot(\mathbf{v}(\mathbf{r}+\mathbf{r}')\times\overline{\mathbf{B}(\mathbf{r}+\mathbf{r}')})\right\rangle. \quad (8)$$

Strong scale separation allows us to neglect terms with derivatives of the large-scale field since such terms will be smaller by the ratio of the eddy scale to the large scale to some power. Consequently we drop terms with derivatives of the large-scale field. Rewriting the expression above we obtain

$$\langle(\mathbf{a}\cdot\overline{\mathbf{B}})\mathbf{v}\rangle+\langle\mathbf{b}\phi_1\rangle=\left\langle\int\frac{d^3\mathbf{r}'}{4\pi r'}(\mathbf{v}(\mathbf{r})\overline{\mathbf{B}(\mathbf{r})}\cdot\mathbf{j}(\mathbf{r}+\mathbf{r}')-\mathbf{b}(\mathbf{r})\overline{\mathbf{B}(\mathbf{r}+\mathbf{r}')}\cdot\omega(\mathbf{r}+\mathbf{r}'))\right\rangle. \quad (9)$$

Following the treatment of Vishniac & Cho (2001), we can substitute $\tau_c(\overline{\mathbf{B}}\cdot\nabla)\mathbf{v}$ for $\mathbf{b}$, where τ_c is the eddy correlation time. This is a reasonable first approximation, but it privileges the velocity field over the magnetic field (we will ultimately include the terms obtained by substituting $-(\overline{\mathbf{B}}\cdot\nabla)\mathbf{b}\tau_c$ for $\mathbf{v}$ in the Appendix). Additionally for an $\alpha-\Omega$ dynamo, we can take $\overline{\mathbf{B}}\approx B_\theta\hat{\theta}$ (cylindrical coordinates ρ,θ,z), and replace $\mathbf{v}$ with its Fourier image. Then we integrate over $\mathbf{r}'$, followed by averaging over $\mathbf{r}$. For a $\hat{z}$-component of (9), this will result in

$$\langle(\mathbf{a}\cdot\overline{\mathbf{B}})v_z\rangle+\langle b_z\phi_1\rangle=-2\tau_c B_\theta^2\int\frac{d^3\mathbf{k}}{(2\pi)^3k^2}\left(k_z v_\rho^*-k_\rho v_z^*\right)k_\theta v_z, \quad (10)$$

where "*" means complex conjugate. Using incompressibility we obtain

$$\langle(\mathbf{a}\cdot\overline{\mathbf{B}})v_z\rangle+\langle b_z\phi_1\rangle=2\tau_c B_\theta^2\int\frac{d^3\mathbf{k}}{(2\pi)^3k^2}\times\left(k_\theta k_\rho\left[\left|v_z^2\right|+\left|v_\rho^2\right|\right]+k_\theta^2\mathrm{Re}\left(v_\rho^*v_\theta\right)\right). \quad (11)$$

This expression is the largest-scale term and does not depend on $\mathbf{r}$. Equation (11) remains mostly unchanged if we go to a shearing system (Cartesian coordinates), since the vertical magnetic field perturbations are not affected by shear ($\Omega=\nabla\times\overline{\mathbf{V}}$) in the horizontal plane.

As discussed by Vishniac & Cho (2001), in order to get a growing magnetic field when $\partial_\rho\Omega<0$ (as in an accretion disk) we need a positive vertical magnetic helicity flux. The first term in (11) at least is guaranteed to have the correct sign in a strongly shearing flow and will reverse sign if the shear is reversed. The second term will have the correct sign if angular momentum transport is outward in accretion disk, and inward in systems with $\partial_\rho\Omega>0$.

Similarly, the vertical component of $\langle\mathbf{b}(\phi_2-\mathbf{a}\cdot\overline{\mathbf{V}})\rangle$ (term 5+6 in Equation (7)) is evaluated in the Appendix with the following result:

$$\langle b_z(\phi_2-\mathbf{a}\cdot\overline{\mathbf{V}})\rangle=-2(r\partial_\rho\Omega)\int\frac{d^3\mathbf{k}}{(2\pi)^3k^4}\times\left[k_\theta^2(|b_z|^2+|b_\theta|^2)-k_\rho^2(|b_\rho|^2+|b_z|^2)\right]. \quad (12)$$

The overall sign of this term is not obvious, but almost certainly depends on how the turbulence is driven. In a strongly shearing flow, where $k_\rho>k_\theta$, increasing $\overline{b_z^2}$ may decrease the effectiveness of the dynamo and lead to the antidynamo behavior. With the opposite sign we get that driving vertical motions, and a stronger vertical field, can add up to the driving forces of the dynamo. For accretion disks ($\Omega\propto r^{-q}$ with $q=3/2$), this term presumably has a negative sign.

We will continue the analysis of expressions (11) and (12) in Section 5, after describing our numerical experiment and its results. So far we can conclude that particular terms of the magnetic helicity flux are sensitive to anisotropy in the turbulence both in real and wave vector spaces. If the information about the relative magnitude of helicity flux terms is initially known, together with degree of turbulence anisotropy, then one can predict whether there is going to be a large-scale dynamo in the system, and whether the dynamo action will be strong or weak.

3. NUMERICAL METHOD

A pseudospectral code is used to solve the incompressible MHD equations in a periodic box of size 2π:

$$\partial\mathbf{V}/\partial t=(\nabla\times\mathbf{V})\times\mathbf{V}-(\nabla\times\mathbf{B})\times\mathbf{B}+\nu\triangle\mathbf{V}+\nabla P'+\mathbf{f} \quad (13)$$

$$\partial\mathbf{B}/\partial t=\nabla\times(\mathbf{V}\times\mathbf{B})+\eta\triangle\mathbf{B} \quad (14)$$

together with $\nabla\cdot\mathbf{V}=0$, $\nabla\cdot\mathbf{B}=0$. Here $P'\equiv P+\mathbf{V}\cdot\mathbf{V}/2$, where P is pressure, $\mathbf{f}$ is forcing, and ν is viscosity. We set $\nu=\eta$. The code was originally written by J. Cho and is described in (Cho & Vishniac 2000). We briefly discuss the details of the simulations below. A fuller description can be found in SV11.

The small-scale turbulence is driven by external forcing term $\mathbf{f}$ in (13), which satisfies $\nabla\cdot\mathbf{f}=0$ and consists of 22 random components. Each of these components has both linearly and circularly polarized parts, the latter can be switched off. Then the forcing becomes non-helical, and the angle of linear polarization of each component performs an independent one-dimensional random walk. The helicity injected into the turbulence in this way is randomly fluctuating with average very close to zero. The forcing correlation time is of the order of the turbulence eddy turnover time at the forcing scale.

The coordinates of each forcing component in k-space are set by a vector $\mathbf{k}_f$. All 22 $\mathbf{k}_f$ are chosen to have equal absolute values $|\mathbf{k}_f|=k_f$ and *one* of the ratios $|\mathbf{k}_{f_i}/k_f|=k_i/k_f$ ($i=x,y,z$; $|k_i/k_f|\in[0;1]$). This means that 22 random forcing components are uniformly applied along the two spherical segments of k-space with radius k_f and fixed k_i/k_f, e.g., for $k_f=15$ with $k_z/k_f=0.8$ and $k_z/k_f=-0.8$.

This forcing with a fixed orientation drives an anisotropic turbulence. For each forcing point, the vector f belongs to a plane orthogonal to $\mathbf{k}_f$. In the 256^3 simulations below we use $k_f=25$ with $k_x/k_f=1$. In this case the turbulence is forced in *YOZ* plane with only a weak component in *X*-direction. At the same time forcing applies highly variable waves along the *X*-direction, while being almost uniform in the *Y*- and *Z*-directions. Thus all three components of the small-scale velocity field (v_x,v_y,v_z) will have strong gradients in the *X*-direction, but not along the other two axes (except as a consequence of nonlinear interactions). The explicit expression for $\mathbf{f}$ and further examples of forcing action are given in SV11.

The initial conditions for the simulations are sinusoidal large-scale shear and a weak seed magnetic field: $V_x=V_0e^{iy}$,

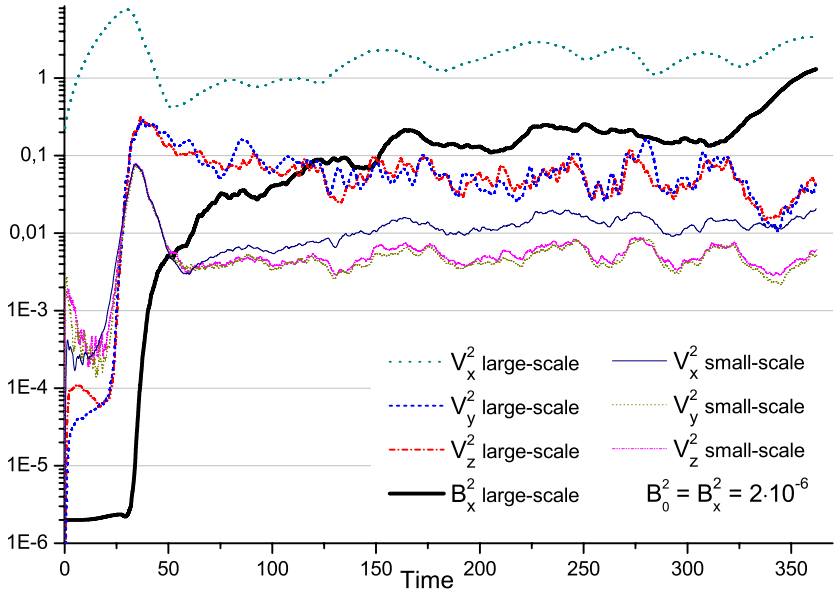

Figure 1. Evolution of the kinetic energy components. Here "large scale" means $k \in [0; 6]$, "small scale" — $k \in [19; 42]$. The shear is supplied by the large-scale V_x, and the eddy turnover time $T_e = 5$–7 (at $k = 25$).

(A color version of this figure is available in the online journal.)

$B_x = B_0 e^{iy}$. $B_0 \sim 10^{-3}$, $V_0 \gg B_0$. V_0 is chosen to satisfy Rossby number $\mathrm{Ro} = k_f v_{k_f}/\overline{V} \approx 1$ and is kept near this value by additional large-scale constant forcing, which supports the shear against dissipation.

For the purposes of this paper we need to compute various triple products, the terms of (6) and (7). Their full spectra exceed the available Fourier space by a factor of three and are truncated. However, these truncations occur several times during the intermediate stages of the computation, and independently for each product. In order to compare various triple products, we have to cut the spectra of initial variables at $k_{\max}/3$. For 256^3, the resolution of our simulations, $k_{\max}/3 = 42$. The forcing scale k_f also has to be kept under $k_{\max}/3$, to include the largest eddies of the turbulence in the data available for triple products. Having forcing under $k = 42$ allows both inertial and dissipative ranges to exist in the interval $[k_f; k_{\max}]$ of the main 256^3 simulation. However, the dynamo action depends only on the largest eddies of the turbulence and resolving the dissipation range is desirable, but generally unimportant.

4. RESULTS

We begin with a simulation of the evolution of the magnetic and velocity fields. This is done once for a particular set of parameters in order to compute the terms of the small-scale magnetic helicity flux (7) and to estimate their relative importance. We choose $\nu = \eta = 7.4 \times 10^{-4}$, an injection scale of the turbulence at $k_f = 25$, $k_x/k = 1$, and with "non-helical" forcing. The Rossby number $\mathrm{Ro} \approx 0.7$–1.2, while the eddy turnover time $T_e \approx 5$–7, and the Reynolds number is $\mathrm{Re} = 2\pi v_{k_f}/k_f \nu \approx 20$–40 (all measured from the simulation). The evolution of velocity and magnetic field amplitudes at various scales is shown in Figures 1 and 2. It was discussed in SV11 in great detail. Here we only note that this set of parameters produces a strong large-scale dynamo in the simulation.

Figure 3 shows the particular terms of divergence of magnetic helicity flux (7). This figure, together with Figures 4 and 5 allows us to analyze various terms based on the averaged absolute values of their totals. "Large scale" means $k \in [0; 6]$, "small scale" means $k \in [19; 42]$ for Figures 1 and 2 only, and we use a sharp split at $k_l = 6.5$ for all other figures: $\overline{\mathbf{B}} = \mathbf{B}(k \leqslant k_l)$ and $\mathbf{b} = \mathbf{B}(k > k_l)$; the particular choice of filtering does not significantly influence our results (see SV11 for details). All terms in Figure 3 are rather well correlated with each other and with the total $\nabla \cdot \mathbf{j}_H$: all of the values of Pearson correlation coefficient r lie in the [0.86; 0.995] interval. We use data only from the time interval [70; 360] to compute r, avoiding its increase during the initial rapid growth of all large-scale quantities. The [70; 360] time interval allows us to study the large-scale dynamo stage without contamination from the earlier small-scale dynamo stage.

The three smallest terms are $\nabla \cdot \overline{\mathbf{b}\phi_s}$ (term 7), $\nabla \cdot \overline{\mathbf{a} \times (\mathbf{v} \times \mathbf{b})}$ (term 8), and $-\nabla \cdot \eta(\overline{\mathbf{a} \times \mathbf{j}})$ (term 9). They can be easily ignored, because their sum contributes less than 3% to the $|\nabla \cdot \mathbf{j}_H|$: the sum of terms 1–6 is equal to the sum of terms 1–9 in Figure 4.

The largest (more than 80% of $\nabla \cdot \mathbf{j}_H$ magnitude) single contribution is given by the fourth term $\nabla \cdot \overline{(\mathbf{a} \cdot \mathbf{b})\overline{\mathbf{V}}}$, due to the large value of the large-scale shear. This term can be approximated by $\nabla \cdot (h\overline{\mathbf{V}})$ with a 15% accuracy. Although this term is large, its relevance to the dynamo process is doubtful. The large-scale shear is not imposed in this simulation, but driven, and consequently fluctuates. This term captures the effect of the large-scale fluctuations in the shear, which creates inhomogeneities along the streamlines. These do not play a significant role in the mean field dynamo. The next largest terms are $\nabla \cdot \overline{\mathbf{b}\phi_2}$ and $-\nabla \cdot \overline{\mathbf{b}(\mathbf{a} \cdot \overline{\mathbf{V}})}$ (5 and 6). They are equal by magnitude (40% of the $|\nabla \cdot \mathbf{j}_H|$ each), but their sum is only about 15% of the $|\nabla \cdot \mathbf{j}_H|$ and it does not contribute to the sum with other terms: $|1 + 2 + 5 + 6| \approx |1 + 2|$ (Figure 4), because the terms 5 and 6 are antiparallel almost everywhere. This is a consequence of the Galilean invariance of the magnetic helicity flux, which leaves only a contribution proportional to the shear, rather than the streaming velocity. We also see that the sum of terms 1–6 is equal to the sum of terms 1–4 in Figure 5. It

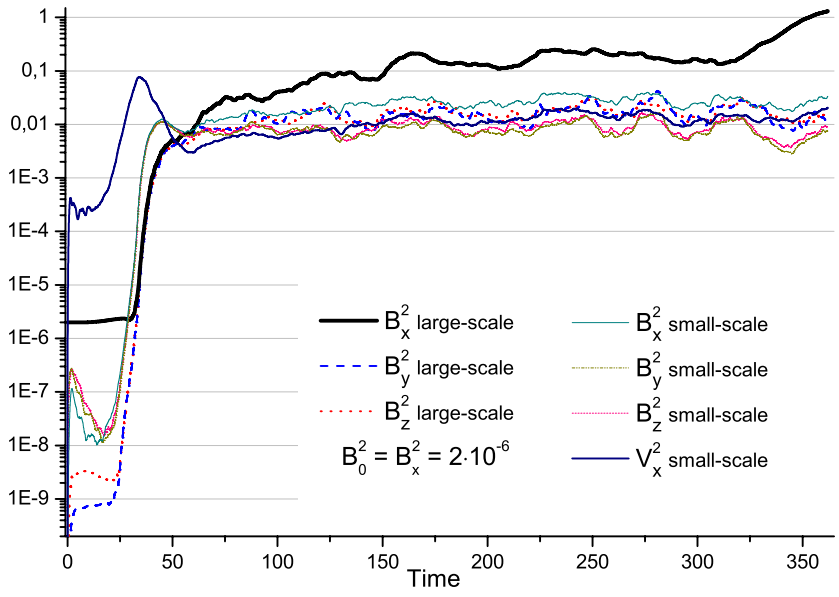

Figure 2. Evolution of the magnetic energy components. Here "large scale" means $k \in [0; 6]$, "small scale" — $k \in [19; 42]$. (A color version of this figure is available in the online journal.)

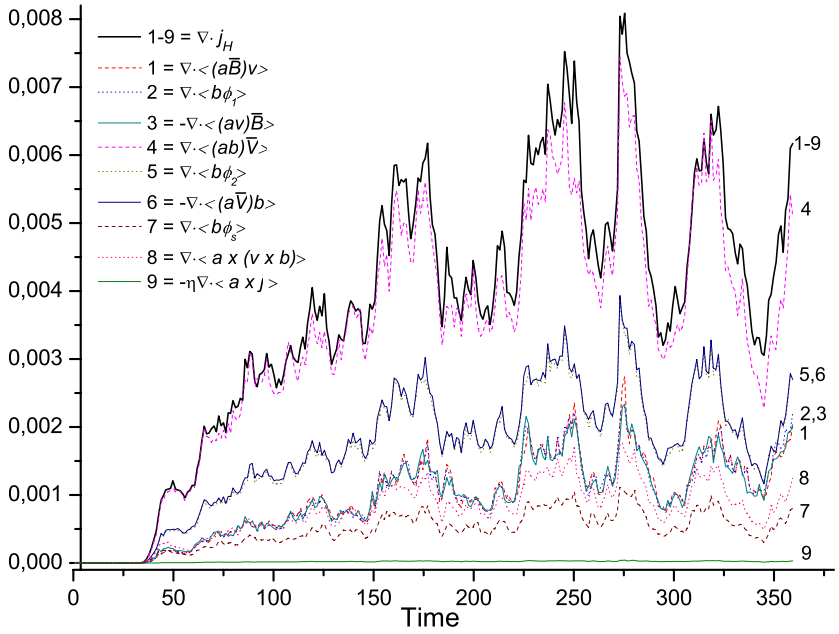

Figure 3. Evolution of particular terms of the divergence of magnetic helicity flux $\nabla \cdot j_H$ (averaged absolute values). For convenience both notations "$\langle\rangle$" and "$\overline{\ }$" are used for large-scale filtering. j_H is defined in Equation (7). Here and in the all following figures "large scale" means $k \in [0; 6.5]$, "small scale" — $k \in (6.5; 42]$. (A color version of this figure is available in the online journal.)

means $\nabla \cdot \overline{\mathbf{b}(\phi_2 - \mathbf{a} \cdot \overline{\mathbf{V}})}$ can be neglected, at least in the given parameter region, i.e., for consideration of the efficient large-scale dynamo. In other situations, e.g., when k_f is much smaller than our $k_f = 25$, the relative importance of this term is expected to increase due to the extra k^{-2} factor in Equation (12), and may be important for antidynamo behavior.

Terms $\nabla \cdot \overline{(\mathbf{a} \cdot \overline{\mathbf{B}})\mathbf{v}}$, $\nabla \cdot \overline{\mathbf{b}\phi_1}$, and $\nabla \cdot \overline{(\mathbf{a} \cdot \mathbf{v})\overline{\mathbf{B}}}$ form the next group in Figure 3. They are also equal by magnitude (20% of $|\nabla \cdot \mathbf{j}_H|$ each). The sum of the first two terms (VC flux) is as large as it can be: $|\mathrm{div}(1 + 2)| \approx |\mathrm{div}(1)| + |\mathrm{div}(2)|$, i.e., the terms 1 and 2 are parallel to each other almost everywhere. This result was discussed in Section 2, after using the approximation $\mathbf{b} \approx \tau_c(\overline{\mathbf{B}} \cdot \nabla)\mathbf{v}$. Now the simulations support the validity of this conclusion. The sum of the first two terms (1 + 2) is the most important contribution to $\nabla \cdot \mathbf{j}_H$ after the advective term $\nabla \cdot \overline{(\mathbf{a} \cdot \mathbf{b})\overline{\mathbf{V}}}$ (ca. 15% of $|\nabla \cdot \mathbf{j}_H|$; see Figure 5). This agrees with the simulations of Arlt & Brandenburg (2001), where the VC flux, driven by the correlation between velocity gradients, was the strongest contributor to the magnetic helicity flux. Also we see that $\overline{(\mathbf{a} \cdot \mathbf{v})\overline{\mathbf{B}}}$ (term 3) can be ignored when compared to the sum of $\overline{(\mathbf{a} \cdot \overline{\mathbf{B}})\mathbf{v}} + \overline{\mathbf{b}\phi_1}$: partial sums (1–6), (1–4), and (1 + 2 + 4) are about the same. Term 3 contributes less than 20% to the partial sum (1 + 2 + 3); the partial sum (3 + 4) approximately equals term 4. Even if term 3 is aligned with the shear, in about half of the points it is antiparallel to it, thus giving no contribution to the sum (3 + 4). However, this term 3 may be

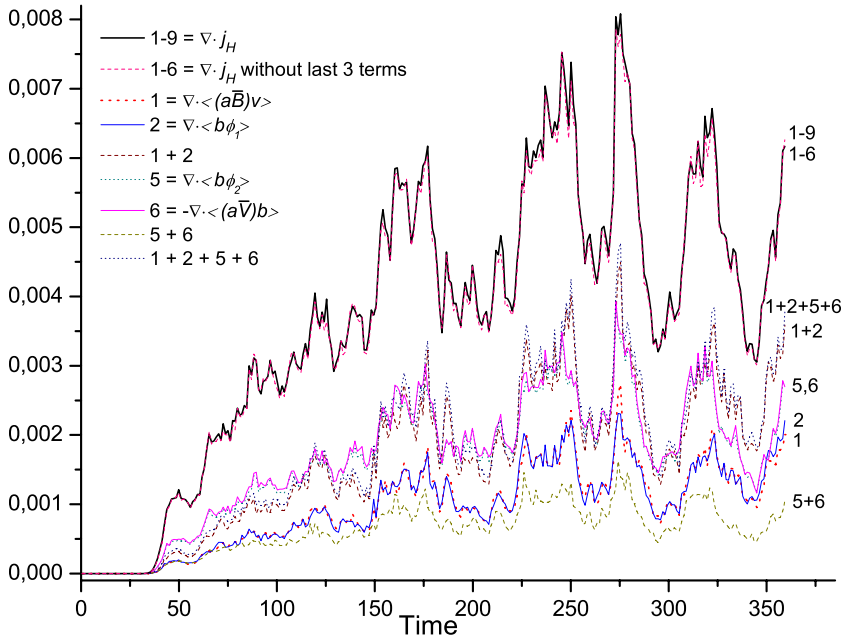

Figure 4. Evolution of particularly interesting combinations of terms in the small-scale magnetic helicity flux $\nabla \cdot j_H$. Both notations "$\langle\rangle$" and "$\overline{\ }$" are used for large-scale filtering.

(A color version of this figure is available in the online journal.)

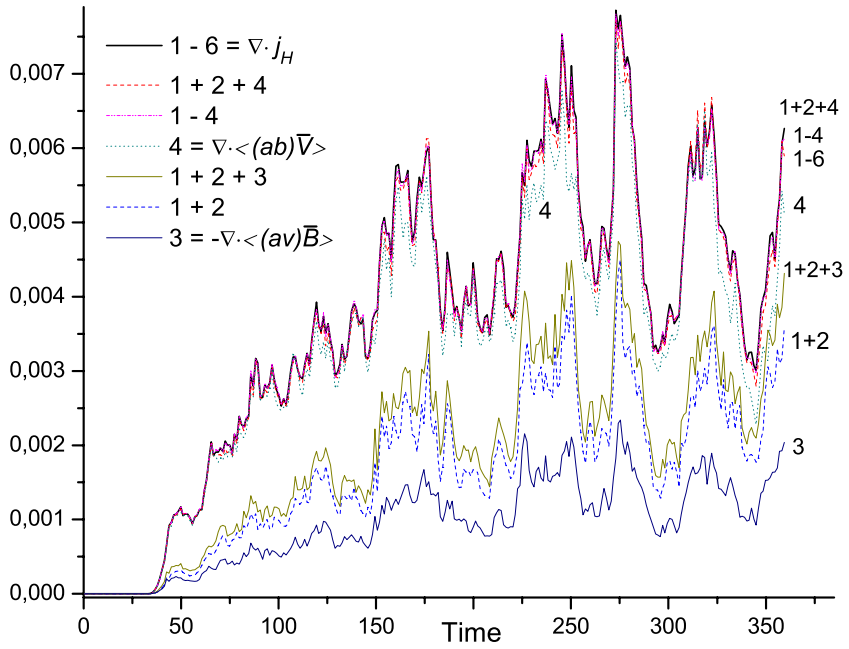

Figure 5. Evolution of another group of combinations of small-scale magnetic helicity flux terms.

(A color version of this figure is available in the online journal.)

oriented differently in other regions of parameter space, but if the $\overline{\mathbf{B}}$ is small, then this term is also small.

Our results show that in efficient large-scale dynamos (more precisely, in the parameter region close to the galactic or solar dynamos) the action of the small-scale magnetic helicity flux $\mathbf{j}_H$ (via its divergence in Equation (6)) can be approximated by

$$j_H = \overline{(\mathbf{a}\cdot\overline{\mathbf{B}})\mathbf{v}} + \overline{\mathbf{b}\phi_1} + \overline{(\mathbf{a}\cdot\mathbf{b})\overline{\mathbf{V}}}, \quad (15)$$

with a very good accuracy (±5% of magnitude), or with a reduced accuracy (±20%), by

$$j_H \simeq 2\overline{(\mathbf{a}\cdot\overline{\mathbf{B}})\mathbf{v}} + h\overline{\mathbf{V}}. \quad (16)$$

The term $\overline{(\mathbf{a}\cdot\mathbf{b})\overline{\mathbf{V}}}$ moves magnetic helicity along the large-scale streamlines, while the VC flux $\overline{(\mathbf{a}\cdot\overline{\mathbf{B}})\mathbf{v}} + \overline{\mathbf{b}\phi_1}$ is responsible for moving magnetic helicity in all other directions, and ultimately for evading the dynamo quenching mechanism.

The importance of the latter term in dynamo process becomes obvious if we compare it with $2\mathcal{E}\cdot\overline{\mathbf{B}}$. Figure 6 demonstrates a very strong correlation between the divergence of the VC flux and $2\mathcal{E}\cdot\overline{\mathbf{B}}$: Pearson $r(1{+}2;\ 2\mathcal{E}\cdot\overline{\mathbf{B}}) = 0.98$. The partial correlation is equally strong; see Table 1. At the same time, Figures 7 and 8 show noticeably worse correlation between term (1 + 2) and both $\partial_t h$ and $\nabla\cdot\overline{(\mathbf{a}\cdot\mathbf{b})\overline{\mathbf{V}}}$ (term 4). The latter two terms happen

Table 1
Degree of Linear Correlation between Various Terms of Equation (6)

	$\nabla\cdot\overline{(\mathbf{a}\cdot\overline{\mathbf{B}})\mathbf{v}}$ (Term 1)	$\nabla\cdot\overline{\mathbf{b}\phi_1}$ (Term 2)	Term (1 + 2)	$\overline{(\mathbf{a}\cdot\mathbf{v})\overline{\mathbf{B}}}$ (Term 3)	$\nabla\cdot\overline{(\mathbf{a}\cdot\mathbf{b})\overline{\mathbf{V}}}$ (Term 4)	$\nabla\cdot(h\overline{\mathbf{V}})$	$\partial_t h$	$\nabla\cdot\overline{\mathbf{b}\phi_2}$ (Term 5)	$\nabla\cdot\overline{\mathbf{b}(\mathbf{a}\cdot\overline{\mathbf{V}})}$ (Term 6)	Term (5 + 6)
$2\mathcal{E}\cdot\overline{\mathbf{B}}$	0.98	0.98	0.98	0.97	0.90	0.90	0.90	0.91	0.91	0.91
$\partial_t h$	0.87	0.88	0.86	0.87	0.97	0.99	1	0.97	0.97	0.93
$\nabla\cdot\overline{(\mathbf{a}\cdot\mathbf{b})\overline{\mathbf{V}}}$	0.87	0.86	0.86	0.88	1	0.98	0.97	0.99	0.99	0.95

Notes. Degree of linear correlation between various terms of Equation (6). We use data from the [70; 360] time interval to compute Pearson's r.

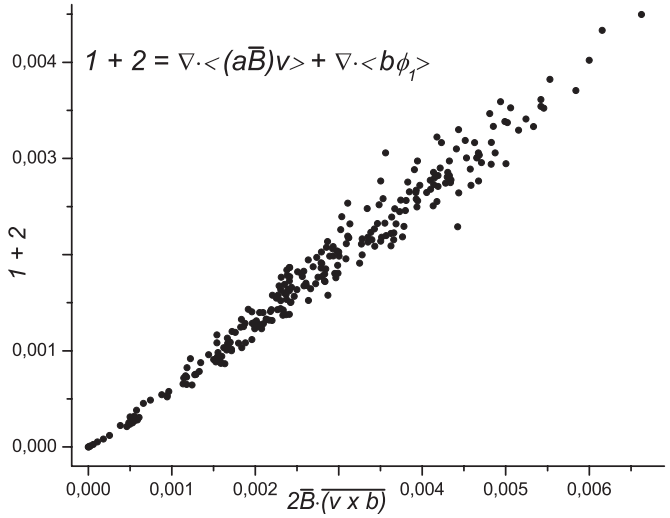

Figure 6. $2\mathcal{E}\cdot\overline{\mathbf{B}}$ (X-axis) plotted against the divergence of the VC flux (term 1 + 2) $\nabla\cdot\overline{(\mathbf{a}\cdot\overline{\mathbf{B}})\mathbf{v}}+\nabla\cdot\overline{\mathbf{b}\phi_1}$ (Y-axis).

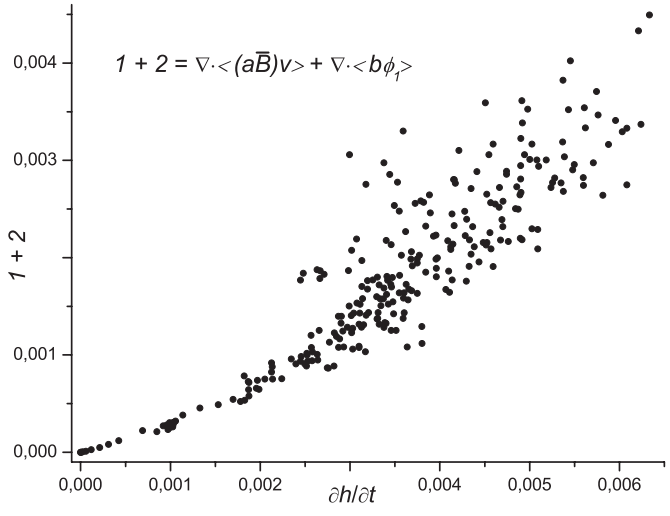

Figure 7. $\partial_t h$ (X-axis) plotted against $\nabla\cdot\overline{(\mathbf{a}\cdot\overline{\mathbf{B}})\mathbf{v}}+\nabla\cdot\overline{\mathbf{b}\phi_1}$ (term 1 + 2, VC flux; Y-axis).

to be very well correlated and even equal each other by overall magnitude (see Figure 9 and Table 1). However, their sum—the Lagrangian derivative of the small-scale magnetic helicity in the large-scale flow $Dh/Dt = \partial_t h + \overline{\mathbf{V}}\cdot\nabla h \approx \partial_t h + \nabla\cdot(h\overline{\mathbf{V}})$—is not small. This follows from the indirect observation that $\partial_t h + \nabla\cdot\mathbf{j}_H$ is much larger than the term $(1+2+3+5+6)$; see Figure 10.

At the same time, terms 5 and 6 together with their sum $\langle\mathbf{b}(\phi_2 - \mathbf{a}\cdot\overline{\mathbf{V}})\rangle$ happen to be well correlated with both term 4 and $\partial_t h$, while being less correlated with $2\mathcal{E}\cdot\overline{\mathbf{B}}$ and term $(1+2)$; see Table 1.

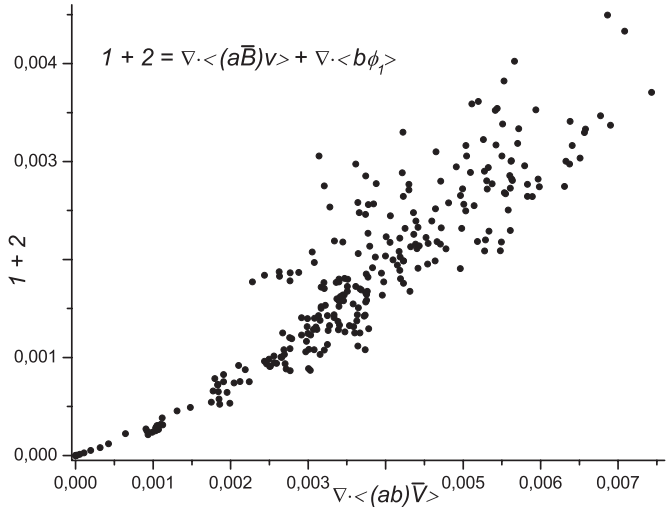

Figure 8. $\nabla\cdot\overline{(\mathbf{a}\cdot\mathbf{b})\overline{\mathbf{V}}}$ (term 4, advective term; X-axis) plotted against $\nabla\cdot\overline{(\mathbf{a}\cdot\overline{\mathbf{B}})\mathbf{v}}+\nabla\cdot\overline{\mathbf{b}\phi_1}$ (term 1 + 2, VC flux; Y-axis).

We can summarize our results by stating that all the important terms of the small-scale magnetic helicity flux can be placed into one of two separate groups: terms 4, 5, and 6 are very well correlated with $\partial_t h$ (and each other) and are not likely to significantly influence the dynamo action, while terms 1, 2, and 3 are very well correlated with $2\mathcal{E}\cdot\overline{\mathbf{B}}$ and, therefore, may be responsible for the large-scale dynamo activity.

5. PREDICTION OF DYNAMO ACTIVITY BASED ON SMALL-SCALE TURBULENCE ANISOTROPY

Considering the apparent importance of the VC flux (term 1 + 2) in the "efficient dynamo" parameter region, and the possible importance of term (5 + 6) in other regions of parameter space, it may be possible to predict the strength of dynamo action using Equations (11) and (12) and some imposed forcing anisotropy. We will compare our results to a set of 64^3 simulations.

Let us consider the term (1+2) first. Equation (11) was derived for an $\alpha-\Omega$ dynamo with cylindrical symmetry ($\overline{\mathbf{B}}\approx B_\theta\hat{\theta}$), while in our simulations $\overline{\mathbf{B}}\approx B_x\hat{x} = B_0 e^{iy}\hat{x}$. Re-deriving terms (1 + 2) from Equation (9), we obtain

$$\langle(\mathbf{a}\cdot\overline{\mathbf{B}})\mathbf{v}\rangle + \langle\mathbf{b}\phi_1\rangle = 2\tau_c B_x^2\int\frac{d^3\mathbf{k}}{(2\pi)^3(k-k_0)^2}\times\left(k_z v_y^* - k_y v_z^* + v_z^*/2\right)k_x\mathbf{v}, \quad (17)$$

where $k_0 = (0, 1, 0)$. This expression is the largest-scale term, which has a spatial dependence only through $B_x = B_0 e^{iy}$.

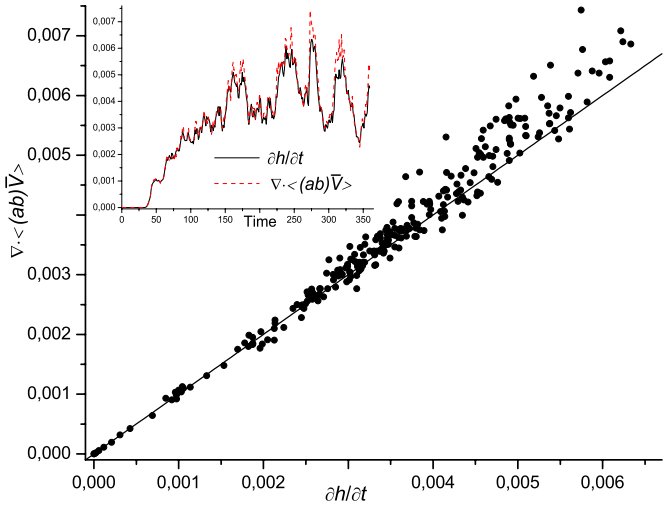

Figure 9. $\partial_t h$ (X-axis) plotted against $\nabla \cdot \overline{(\mathbf{a}\cdot\mathbf{b})\overline{\mathbf{V}}}$ (term 4, advective term; Y-axis). Straight line is $y = x$. The inset shows the time evolution of both quantities.

(A color version of this figure is available in the online journal.)

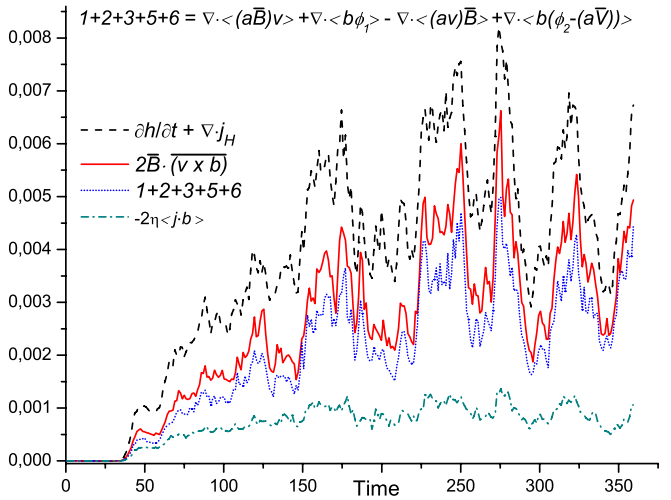

Figure 10. Evolution of the terms of Equation (6). For comparison, the dissipative term $-2\eta\overline{\mathbf{j}\cdot\mathbf{b}}$ is also shown. If the Lagrangian derivative $\partial_t h+\nabla\cdot(h\overline{\mathbf{V}})$ is small, then $\partial_t h+\nabla\cdot\mathbf{j}_H = \partial_t h+1+2+3+4+5+6$ should be close to 1+2+3+5+6.

(A color version of this figure is available in the online journal.)

The largest-scale term of its divergence would then depend on $(1+2)_y$, which can be transformed using incompressibility:

$$\langle(\mathbf{a}\cdot\overline{\mathbf{B}})v_y\rangle + \langle b_y\phi_1\rangle = \tau_c B_x^2 \int \frac{d^3\mathbf{k}}{(2\pi)^3(k-k_0)^2} \times \left(k_x k_z\left[|v_y^2| + |v_z^2|\right] + k_x^2\mathrm{Re}(v_z^* v_x) + k_x\mathrm{Re}(v_z^* v_y)/2\right). \quad (18)$$

We clearly see from either (11) or (18) that the magnitude of the term depends on a small-scale velocity anisotropy, both in real and Fourier spaces, providing an analytical answer to the question of how forcing anisotropy, or more generally—the anisotropy of the MHD turbulence influences dynamo action. However, it is not straightforward to relate (18) to the forcing function used in our simulations. The small-scale velocity is 0 by definition at large scales, i.e., the factor $(k-k_0)^{-2} \approx k^{-2}$ is not strongly influencing the overall expression. If we force the small-scale velocity field only at particular points in k-space, the other points will have smaller magnitude and may be neglected. Then the integral over k-space in (18) can be approximated by the sum just over the forcing points. If the forcing is oriented in some direction then this means that the velocity is highly periodic in this direction (e.g., for $k_x/k_f = 1$ along X) and near-uniform functions are applied in the other two directions. At the same time, the chosen orientation means that forcing amplitude in this direction is much smaller than in the orthogonal directions. For instance, $k_x/k_f = 1$ would result in $v_x \ll v_y, v_z$. Also we can suppose that term $k_x^2\mathrm{Re}(v_z^* v_x)$ in (18) is more important than $k_x k_z[|v_y^2| + |v_z^2|]$, because we choose forcing points symmetrically around the origin of k-space, and the equal quantities of terms with opposite signs are likely to mostly cancel each other.

Consequently, different forcing orientations would translate via Equation (18) into the strongest large-scale dynamo for a $k_z/k_f = 1$ (due to the contribution of the first term in (18)), strong to moderate dynamo for $k_x/k_f = 1$ (due to third term in (18)) and a weaker dynamo for $k_y/k_f = 1$. Intermediate forcing orientations (one of $k_x/k_f, k_y/k_f, k_z/k_f \approx 0.5$) will also produce a dynamo, due to all three components of velocity being far from zero and about equal in magnitude. For $k_x/k_f = 0.5$ the dynamo would be stronger than for $k_x/k_f = 1$, due to the large k_x^2 factor at $k_x^2\mathrm{Re}(v_z^* v_x)$. A forcing orientation $k_x/k_f = 0$ will produce no dynamo, because of the $k_x = 0$ factor in front of every term in (18), but $k_y/k_f = 0$ will result in a moderate dynamo (both the third term and $|v_y^2|$ are quite large). $k_z/k_f = 0$ will produce a weaker dynamo, because only the third term will be large. This analysis is oversimplified, but it is an adequate illustration of how the forcing anisotropy may work.

The actual simulation data are given in Table 2. For various forcing orientations we calculated large-scale magnetic field at $T = 250$ (100,000 iterations at 64^3), which is well inside the large-scale dynamo stage, with magnitude of magnetic field indicating the overall dynamo strength. In all cases the largest component of magnetic field was B_x. The theoretical predictions given above are in general agreement with the simulation results from Table 2; however, there are some notable discrepancies, e.g., the actual absence of a large-scale dynamo at $k_z/k_f = 0$ and different relative strengths of the dynamo at various k_i/k_f.

Now let us consider the term 5 + 6 (Equation (12)). This term of small-scale magnetic helicity flux has an extra k^{-2} factor in comparison with (11) or (18), i.e., it should be less significant, especially when the majority of the magnetic energy is concentrated at small scales. Its magnitude should grow while increasing the forcing scale toward $k = 0$. This may be the reason for antidynamo action becoming stronger for smaller k_f (for accretion disks this term is expected to be negative). Using similar reasoning as for term (1 + 2), we can predict that in our simulations forcing with $k_z/k_f = 1$ would make term (5 + 6) relatively small (due to low values of k_x, k_y), while $k_z/k_f = 0$ would lead to an opposite situation, increasing the magnitude of this term. At the same time our numerical simulations show that the antidynamo becomes stronger when $k_z/k \to 0$ (at $k_f \approx 2$–15), while just the small-scale dynamo is observed when $k_z/k \to 1$ for the same range of k_f. This phenomenon may be related to the observation that (for $k_f \approx 20$ and up) the strongest large-scale dynamo is at $k_z/k_f = 1$ and it vanishes for $k_z/k_f = 0$, due to the negative contribution from term (5 + 6) to the small-scale magnetic helicity flux.

We conclude that Equations (11), (18), and k_f — (12) — lead for low to qualitatively correct predictions about the presence of a large-scale dynamo or antidynamo. However, detailed

Table 2
Dependence of Large-Scale Dynamo Strength on Small-Scale Forcing Orientation

Forcing orientation	$k_x/k_f = 1$	$k_x/k_f = 0.5$	$k_x/k_f = 0$	$k_y/k_f = 1$	$k_y/k_f = 0.5$	$k_y/k_f = 0$	$k_z/k_f = 1$	$k_z/k_f = 0.5$	$k_z/k_f = 0$
$\lvert B_x\rvert$ at $T = 250$	0.12	0.33	No LS dynamo	0.2	0.17	0.42	0.87	0.6	No LS dynamo

Notes. Dependence of large-scale dynamo strength on small-scale forcing orientation. The resolution is 64^3, $k_f = 25$.

predictions of dynamo strength will require a more detailed and complicated analysis of these equations to be reliable.

6. CONCLUSIONS

In this paper, we have presented theoretical and numerical analysis of the small-scale magnetic helicity flux in MHD turbulence leading to a large-scale dynamo. This flux consists of up to nine distinct terms, but in the simulated region of parameter space (close to galactic or solar dynamos), only two of these terms turn out to be important. Together they comprise more than 95% of the divergence of the flux by magnitude. The largest term $\overline{(\mathbf{a}\cdot\mathbf{b})\overline{\mathbf{V}}}$ is responsible for advective motion of small-scale magnetic helicity with large-scale velocity and does not contribute to the dynamo action. The smaller term $\overline{(\mathbf{a}\cdot\overline{\mathbf{B}})\mathbf{v}} + \overline{\mathbf{b}\phi_1}$, the so-called VC flux, may be directed across large-scale velocity and magnetic field lines and is very highly correlated with the parallel component of the turbulent e.m.f. This term prevents local excess accumulation of magnetic helicity of the incorrect sign (and dynamo quenching), i.e., it is likely be responsible for large-scale dynamo action. All the other terms of the magnetic helicity flux are negligible. However, some of them may become important in other regions of parameter space. The most interesting one is $\overline{\mathbf{b}(\phi_2 - \mathbf{a}\cdot\overline{\mathbf{V}})}$, which is likely to be the key for antidynamo action.

To study the influence of MHD turbulence anisotropy on dynamo and considering the significance of VC flux and "antidynamo term," we derived analytical expressions for them solely in terms of small-scale velocity and separately—in terms of small-scale magnetic field. These expressions clearly show how the particular anisotropy may change the each term and possibly—the dynamo action. We were able to predict the existence of a large-scale dynamo and its strength using straightforward estimates of the magnitude of the VC flux for different orientations of the small-scale forcing. These predictions agreed with simulation results in most cases. Similarly, for systems with forcing close to the largest scales we were able to predict the observed dependence of the antidynamo strength on forcing anisotropy. A more detailed analysis of these terms in the magnetic helicity flux, tailored for particular system geometry, would lead to deeper and more accurate predictions of dynamo action in the future.

We are happy to acknowledge the important role Jungyeon Cho played in producing the simulations we presented here. This work was supported by the National Science Foundation under ITR:AST-0428325 and by the National Science and Engineering Research Council of Canada and utilized a Linux cluster of the Physics & Astronomy Department at Johns Hopkins University.

APPENDIX

EVALUATION OF CERTAIN TERMS OF THE MAGNETIC HELICITY FLUX

In this Appendix, we first evaluate $\langle\mathbf{b}(\phi_2 - \mathbf{a}\cdot\overline{\mathbf{V}})\rangle$—the sum of the fifth and sixth terms in Equation (7)—using the same approach as for Equations (8)–(11). We rewrite the term as an integral over correlations:

$$(\phi_2 - \mathbf{a}\cdot\overline{\mathbf{V}}) = \int \frac{d^3\mathbf{r}'}{4\pi r'}[-\nabla\cdot(\overline{\mathbf{V}(\mathbf{r}+\mathbf{r}')}\times\mathbf{b}(\mathbf{r}+\mathbf{r}')) - \overline{\mathbf{V}(\mathbf{r})}\cdot\mathbf{j}(\mathbf{r}+\mathbf{r}')]. \quad \text{(A1)}$$

Here we will not immediately neglect the derivative of the large-scale velocity, since the leading order term will depend on it. We write

$$\overline{V_i(\mathbf{r}+\mathbf{r}')} = \overline{V_i(\mathbf{r})} + r'_m\partial_m\overline{V_i} = \overline{V_i(\mathbf{r})} + r'_m\left(\sigma_{mi} + \frac{1}{2}\epsilon_{mil}\overline{W_l}\right), \quad \text{(A2)}$$

where σ_{mi} is the symmetrical part of the shear tensor and $\overline{\mathbf{W}}$ is the vorticity of the large-scale velocity field. Using this, the integrand in (A1) can be rewritten as $-\partial_j[\epsilon_{jik}r'_m(\sigma_{mi} + \epsilon_{mil}\overline{W_l}/2)b_k(\mathbf{r}+\mathbf{r}')]/4\pi r'$, and after integrating by parts further reduced to $[\sigma_{mi}\epsilon_{jik}(\partial_m\partial_j r') - \overline{W_l}\partial_l\partial_k r'/2]b_k(\mathbf{r}+\mathbf{r}')/4\pi$. We expect the last term to vanish, since there is unlikely to be a contribution from solid-body rotation. This is true after another integration by parts, since $\nabla\cdot\mathbf{b} = 0$. We can rewrite the magnetic helicity flux from the term 5 + 6 in Equation (7) as

$$\langle\mathbf{b}(\phi_2 - \mathbf{a}\cdot\overline{\mathbf{V}})\rangle = \langle\partial_m\mathbf{b}(\mathbf{r})\int r'\frac{d^3\mathbf{r}'}{4\pi}\sigma_{mi}\,j_i(\mathbf{r}+\mathbf{r}')\rangle. \quad \text{(A3)}$$

The integral operator here is equivalent to $-2\nabla^{-4}$. We can use this fact to rewrite the contribution to the vertical magnetic helicity flux as

$$\langle b_z(\phi_2 - \mathbf{a}\cdot\overline{\mathbf{V}})\rangle = -2(r\partial_\rho\Omega)\int\frac{d^3\mathbf{k}}{(2\pi)^3k^4} \times\left[k_\theta^2(|b_z|^2 + |b_\theta|^2) - k_\rho^2(|b_\rho|^2 + |b_z|^2)\right]. \quad \text{(A4)}$$

Comparing $\langle(\mathbf{a}\cdot\overline{\mathbf{B}})\mathbf{v}\rangle + \langle\mathbf{b}\phi_1\rangle$ in Equation (11) with (A4), we see several differences. The Equation (11) depends on correlations between different directions and includes an approximate integration over time. The Equation (A4) includes neither but depends on differences in the mean square field in different directions at different wavenumbers. The integration over time in the derivation of Equation (11) is particularly problematic, with a clear need to redo it to include the effects of shear.

We also note that expressing $\mathbf{b}$ in terms of $\mathbf{v}$, or vice versa, is badly motivated. We could do either, and in doing so we use different dynamical equations, and arrive at different expressions. The more correct approach is to consider the growth of a quadratic expression from zero, i.e., take the derivative and multiply by the τ_c. This is equivalent to adding together the results of substituting $\mathbf{v}$ for $\mathbf{b}$ and vice versa. More concretely, consider the usual expression for the e.m.f., $\overline{\mathbf{v}\times\mathbf{b}}$. If this is zero at some moment in time, we can approximate its value at later times by retaining only quadratic perturbation quantities, i.e.,

$$\overline{(\mathbf{v}\times\mathbf{b})_i} \approx \tau_c\partial_t\overline{(\mathbf{v}\times\mathbf{b})_i} = (-\alpha_{ij} + h_{ij})\overline{B}_j\tau_c, \quad \text{(A5)}$$

where α_{ij} and h_{ij} are the kinetic and current helicity tensors, respectively. This approach is similar to the one employed in the MFT. Applying the same line of reasoning to evaluating the magnetic helicity flux, the right part of Equation (9) becomes

$$-2\left\langle \int \frac{d^3\mathbf{r}'}{4\pi r'}[\omega(\mathbf{r}+\mathbf{r}')\cdot\overline{\mathbf{B}}(\overline{\mathbf{B}}\cdot\nabla)\mathbf{v}(\mathbf{r}) - \mathbf{j}(\mathbf{r}+\mathbf{r}')\cdot\overline{\mathbf{B}}(\overline{\mathbf{B}}\cdot\nabla)\mathbf{b}(\mathbf{r})]\right\rangle\tau_c. \quad \text{(A6)}$$

Substituting $\mathbf{v}$ for $\mathbf{b}$ in the shearing system will result in long derivations. Leaving them aside, below we provide only the vertical component of the first two terms of j_H in Equation (7), which is supposed to play a critical role in the $\alpha-\Omega$ dynamo. The magnetic back-reaction contribution to the first term in (9) is $\langle \overline{B}_\theta j_\theta v_z\rangle \approx \overline{B}_\theta \langle j_\theta v_z\rangle$ (we again assume $\overline{\mathbf{B}} \approx B_\theta\hat{\theta}$ for the $\alpha-\Omega$ dynamo),

$$\overline{B}_\theta\langle j_\theta v_z\rangle = \frac{\tau_c\overline{B}_\theta^2}{1+N^2\tau_c^2}\cdot\Bigg[-\left(k_\theta^2\overline{b_\rho b_\theta}+k_\rho k_\theta\left(\overline{b_\rho^2}+\overline{b_z^2}\right)\right) \times\left[1-\frac{k_z^2}{Q}(\kappa^2-N^2)\tau_c^2\right]+\frac{\Omega\tau_c}{Q}\Big[\left(k_\rho^2+k_z^2\right)(2-q)k_\theta^2\overline{b_\rho^2} + k_\rho k_\theta\Big(-2\left(k_\rho^2+k_z^2\right)+(2-q)k_\theta^2\Big)\overline{b_\rho b_\theta}-2k_\rho^2k_\theta^2\overline{b_\theta^2}\Big]\Bigg], \quad \text{(A7)}$$

where $\kappa^2\equiv 2(2-q)\Omega^2$, $\Omega\propto\rho^{-q}$, $q=3/2$ (in accretion disk), N is the buoyancy frequency,

$$Q=\frac{k_\rho^2+k_\theta^2+q\Omega\tau_c k_\rho k_\theta}{1+\kappa^2\tau_c^2}+\frac{k_z^2}{1+N^2\tau_c^2}. \quad \text{(A8)}$$

In the absence of shear, $-\langle b_z\overline{B}_\theta\omega_\theta\rangle$, the second term in (9) gives the same contribution.

For a nonzero shear we can integrate by parts, assume incompressibility, and obtain

$$-\langle b_z\overline{B}_\theta\omega_\theta\rangle = \overline{B}_\theta(\overline{j_\theta v_z}-\overline{b_\rho\partial_\theta v_\theta}+\overline{b_\theta\partial_\theta v_\rho}). \quad \text{(A9)}$$

The first term in (A9) just gives us a repetition of Equation (A7). The last two terms are

$$\begin{aligned}\overline{B}_\theta[\overline{b_\theta\partial_\theta v_\rho}-\overline{b_\rho\partial_\theta v_\theta}] &= \overline{B}_\theta^2k_\theta^2\tau_c\Bigg[\frac{-\overline{b_\rho b_\theta}}{\left(1+N^2\tau_c^2\right)Q}\left((4-q)\Omega\tau_c k_\rho k_\theta+N^2\tau_c^2\left(k_\theta^2-k_\rho^2\right)\right) \\ &+\frac{\overline{b_\theta^2}}{1+\kappa^2\tau_c^2}\left(-2\Omega\tau_c+\frac{k_\rho+2\Omega\tau_c k_\theta}{Q}\times\left[2\Omega\tau_c k_\rho-k_\theta\frac{(\kappa^2-N^2)\tau_c^2}{1+N^2\tau_c^2}\right]\right) \\ &+\frac{\overline{b_\rho^2}}{1+\kappa^2\tau_c^2}\left((q-2)\Omega\tau_c+\frac{k_\theta-(2-q)\Omega\tau_c k_\rho}{Q}\times\left[k_\theta(2-q)\Omega\tau_c+k_\rho\frac{(\kappa^2-N^2)\tau_c^2}{1+N^2\tau_c^2}\right]\right)\Bigg]. \quad \text{(A10)}\end{aligned}$$

REFERENCES

Arlt, R., & Brandenburg, A. 2001, A&A, 380, 359
Berger, M. A. 1984, GApFD, 30, 79
Berger, M. A. 1997, JGR, 102, 2637
Blackman, E. G., & Field, G. 2002, PhRvL, 89, 265007
Brandenburg, A. 2005, in Cosmic Magnetic Fields, ed. R. Wielebinski & R. Beck (Lecture Notes in Physics, Vol. 664; Berlin: Springer), 219
Brandenburg, A., & Subramanian, K. 2005a, PhR, 417, 1
Brandenburg, A., & Subramanian, K. 2005b, AN, 326, 400
Cho, J., & Vishniac, E. T. 2000, ApJ, 538, 217
Démoulin, P., Mandrini, C. H., van Driel-Gesztelyi, L., et al. 2002, A&A, 382, 650
Frisch, U., Pouquet, A., Léorat, J., & Mazure, A. 1975, JFM, 68, 769
Gruzinov, A. V., & Diamond, P. H. 1994, PhRvL, 72, 1651
Kleeorin, N., Moss, D., & Rogachevskii, I. 2000, A&A, 361, L5
Kleeorin, N., & Ruzmaikin, A. 1982, MHD, 18, 116
Lynch, B. J., Gruesbeck, J. R., Zurbuchen, T. H., & Antiochos, S. K. 2005, JGR, 110, A08107
Pouquet, A., Frisch, U., & Léorat, J. 1976, JFM, 77, 321
Shapovalov, D., & Vishniac, E. T. 2011, ApJ, 738, 66
Shukurov, A., Sokoloff, D., Subramanian, K., & Brandenburg, A. 2006, A&A, 448, L33
Steenbeck, M., Krause, F., & Rädler, K.-H. 1966, ZNatA, 21, 369
Subramanian, K., & Brandenburg, A. 2006, ApJL, 648, L71
Subramanian, K., Shukurov, A., & Haugen, N. E. L. 2006, MNRAS, 366, 1437
Sur, S., Shukurov, A., & Subramanian, K. 2007, MNRAS, 377, 874
Taylor, J. B. 1974, PhRvL, 33, 1139
Vishniac, E. T., & Cho, J. 2001, ApJ, 550, 752